Supramolecular Approaches to Second-Order Nonlinear Optical Materials. Self-Assembly and Microstructural Characterization of Intrinsically Acentric [(Aminophenyl)azo]pyridinium Superlattices

Wenbin Lin,[†] Weiping Lin,[‡] George K. Wong,[‡] and Tobin J. Marks*,[†]

Contribution from the Department of Chemistry, the Department of Physics and Astronomy, and the Materials Research Center, Northwestern University, Evanston, Illinois 60208-3113

Received February 7, 1996[⊗]

Abstract: This paper describes the synthesis and characterization of self-assembled second-order nonlinear optical multilayer materials containing the high-hyperpolarizability [(aminophenyl)azo]pyridinium chromophore. The chromophoric multilayers are assembled on clean glass or single-crystal silicon substrates via the following iterative reaction sequence: (1) treatment with 4-$ClCH_2C_6H_4SiCl_3$, 3-$BrC_3H_6SiCl_3$, or 3-$IC_3H_6SiCl_3$ to afford a self-assembled coupling layer; (2) quaternization of 4-[[4-[*N*,*N*-bis(hydroxylethyl)amino]phenyl]azo]pyridine in a "topotactic" fashion to generate an [(aminophenyl)azo]pyridinium chromophore layer; (3) cross-linking with octachlorotrisiloxane to afford a capping layer (which also regenerates surface hydroxyl groups for subsequent layer deposition). The new chromophore precursor 4-[[4-[*N*,*N*-bis(hydroxylethyl)-amino]phenyl]azo]pyridine was synthesized by diazotization of 4-aminopyridine followed by coupling with *N*-phenyldiethanolamine and has been characterized by elemental analysis, mass spectrometry, and infrared, UV−vis, and NMR spectroscopies. The chromophoric multilayers have been characterized by X-ray photoelectron and transmission optical spectroscopies, spectroscopic ellipsometry, X-ray reflectivity, advancing contact angle measurements, and polarized second harmonic generation (SHG). The excellent structural regularity of the chromophoric multilayers is indicated by the linear dependence of the [(aminophenyl)-azo]pyridinium chromophore longitudinal HOMO → LUMO charge-transfer excitation absorbance at 572 nm and the ellipsometry- and X-ray reflectivity-derived multilayer thicknesses on the number of assembled trilayers, while the uniform polar order of the stacked chromophoric multilayers is evidenced by the quadratic dependence of the second harmonic generation intensities on the number of trilayers. The [(aminophenyl)azo]pyridinium multilayers are photochemically stable, have very high structural regularities, and exhibit a second-order nonlinear optical susceptibility ($\chi^{(2)}$) of $\sim 3.6 \times 10^{-7}$ esu ($\sim$150 pm/V) at a fundamental wavelength of 1064 nm. Finally, atomic force microscopy reveals that the surfaces of the self-assembled multilayers are very smooth (root mean square roughness = 12 Å for a 10 trilayer sample), undoubtedly reflecting the high three-dimensional structural regularities of the individual layers.

Introduction

There is great current fundamental scientific and technological interest in the synthesis and properties of molecule-based materials having large second-order optical nonlinearities because they present special conceptual synthetic challenges and because of their potential applications in second harmonic generation (SHG), electrooptic, and photorefractive devices.[1] Molecule-based second-order nonlinear optical materials offer many attractions, such as large nonresonant response, ultrafast response times, low dielectric constants/losses, and intrinsic architectural tailorability.[2] Because second-order nonlinear optical susceptibility is a third rank tensor, the effect vanishes if the constituent molecular chromophores are arranged in a centrosymmetric architecture.[3] Therefore, noncentrosymmetric organization of high molecular hyperpolarizability constituent chromophores is an essential requirement for efficient bulk second-order nonlinear optical materials, and the construction of such acentric supramolecular assemblies presents a daunting challenge to conventional synthetic methodologies.[4] Of these, poled polymer[2b,c] and Langmuir−Blodgett (LB) film transfer approaches[5] have been most commonly employed to prepare second-order nonlinear optical materials. Although considerable progress has been made in the fabrication of noncentrosymmetric assemblies via the above two approaches in recent years, significant synthetic challenges still remain and have thus far impeded the realization of optimum materials.[2b,c,5] Molecular self-assembly is an attractive alternative approach to second-order NLO materials and targets the construction of covalently linked, intrinsically acentric superlattices containing molecular chromophoric subunits.[6,7]

The field of molecular self-assembly has witnessed tremendous growth in synthetic sophistication and depth of charac-

[†] Department of Chemistry.
[‡] Department of Physics and Astronomy.
[⊗] Abstract published in *Advance ACS Abstracts,* August 1, 1996.

(1) (a) Moerner, W. E.; Silence, S. M. *Chem. Rev.* **1994**, *94*, 127−155. (b) Dalton, L. R.; Harper, A. W.; Ghosn, R.; Steier, W. H.; Ziari, M.; Fetterman, H.; Shi, Y.; Mustacich, R. V.; Jen, A. K.-Y.; Shea, K. J. *Chem. Mater.* **1995**, *7*, 1060−1081. (c) Dalton, L. R.; Harper, A. W.; Wu, B.; Ghosn, R.; Laquindanum, J.; Liang, Z.; Hubbel, A.; Xu, C. *Adv. Mater.* **1995**, *7*, 519−540. (d) Marder, S. R.; Sohn, J. E.; Stucky, G. D. *Materials for Nonlinear Optics*; ACS Symposium Series 455; American Chemical Society: Washington, DC, 1991.

(2) (a) Kanis, D. R.; Ratner, M. A.; Marks, T. J. *Chem. Rev.* **1994**, *94*, 195−242. (b) Marks, T. J.; Ratner, M. A. *Angew. Chem., Int. Ed. Engl.* **1995**, *34*, 155−173 and references therein. (c) Burland, D. M.; Miller, R. D.; Walsh, C. A. *Chem. Rev.* **1994**, *94*, 31−75.

(3) Prasad, P. N.; Williams, D. J. *Introduction to Nonlinear Optical Effects in Molecules and Polymers*; John Wiley & Sons: New York, 1991; Chapter 4.

(4) Lehn, J.-M. *Angew. Chem., Int. Ed. Engl.* **1988**, *27*, 89−112.

(5) (a) Ashwell, G. J.; Jackson, P. D.; Crossland, W. A. *Nature* **1994**, *368*, 438−440. (b) Penner, T. L.; Matschmann, H. R.; Armstrong, N. J.; Ezenyilimba, M. C.; Williams, D. J. *Nature* **1994**, *367*, 49−51. (c) Ashwell, G. J.; Hargreaves, R. C.; Baldwin, C. E.; Bahra, G. S.; Brown, C. R. *Nature* **1992**, *357*, 393−395.

S0002-7863(96)00395-2 CCC: $12.00 © 1996 American Chemical Society

terization over the past decade.[8] Numerous self-assembled systems have been investigated, including disulfides and thiols on gold,[9] carboxylic acids on metal oxides,[10] trichloro- and trialkoxysilanes on oxides,[11] and phosphonates on metal phosphonate surfaces.[7,12] Spontaneous and sequential adsorption of appropriately derivatized adsorbates onto substrates in a self-limiting fashion can yield thin films with uniform polar orders in individual layers and therefore represents an attractive approach to the construction of intrinsically acentric chromophoric superlattices. Unfortunately, while the routes to self-assembled *monolayers* are very well developed, few efficient routes to structurally regular self-assembled *multilayers* have been devised.[13] Among them, self-assembled siloxane and metal phosphonate systems are promising candidates for constructing acentric superlattices. Several years ago, we reported synthetic routes to the first SHG-active multilayer structures using an attractive covalent siloxane self-assembly approach; highly regular and highly nonlinear ($\chi^{(2)} \sim 200$ pm/V at $\omega_0 = 1064$ nm) self-assembled stilbazolium (**I**) multilayers were constructed in a regular, layer-by-layer fashion.[6a] Katz *et al*. later showed that acentric chromophoric multilayers could also be obtained using a zirconium phosphate/phosphonate self-assembly approach.[7]

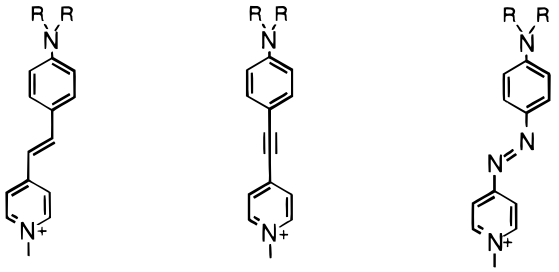

I **II** **III**

Recently, we reported a new "topotactic" pathway for the preparation of self-assembled stilbazolium (**I**) and [(aminophenyl)ethynyl]pyridinium (**II**) multilayers with greatly improved synthetic efficiency, structural regularity, and second-order nonlinear optical response.[14] A full account of the synthesis, microstructures, and NLO response characteristics of these materials will be presented elsewhere.[14d] Our studies also indicated that both the chemical and photophysical properties of these self-assembled materials strongly depend on the chromophore molecular architectures. For example, the stilbazolium monolayers not only exhibit packing geometries very different from those of the [(aminophenyl)ethynyl]pyridinium monolayers[15] but also exhibit $\chi^{(2)}$ responses up to 10× larger than those of the latter.[6c,15] Therefore, it would be of great interest to investigate the properties of self-assembled superlattices in which the chromophore conjugative pathway, hyperpolarizability, shape, and potential chemical/photochemical reactivity were further modified. To this end, we have designed a new [(aminophenyl)azo]pyridinium chromophore (**III**) for incorporation into siloxane self-assembled multilayer structures. This azo chromophore can potentially exhibit additional advantages such as enhanced thermal, oxidative, and photochemical stability. For example, previous studies have suggested that diphenylazo NLO chromophores are more thermally stable than the stilbene analogs.[16] In addition, the [(aminophenyl)azo]-pyridinium molecules should be resistant to degradative [2 + 2] cycloaddition pathways that are potential complications in some stilbazolium systems and that would result in diminished NLO activity.[17] We present in this paper the synthesis of the new [(aminophenyl)azo]pyridine chromophore precursor and its efficient self-assembly into [(aminophenyl)azo]pyridinium superlattices. We report detailed characterization of these self-assembled [(aminophenyl)azo]pyridinium mono- and mutlilayers using X-ray photoelectron and transmission optical spectroscopies, spectroscopic ellipsometry, X-ray reflectivity, advancing contact angle measurements, and polarized second harmonic generation (SHG) measurements. It will be seen that these readily synthesized superlattices exhibit very high second-order nonlinear response and high structural regularity as well as high chemical/photochemical stability.[18]

Experimental Section

The synthesis, purification, and characterization of the reagents (3-iodopropyl)trichlorosilane (3-$IC_3H_6SiCl_3$) and 4-[[4-[*N*,*N*-bis(hydroxylethyl)amino]phenyl]azo]pyridine can be found in the supporting information.

(6) (a) Li, D.; Ratner, M. A.; Marks, T. J.; Zhang, C.; Yang, J.; Wong, G. K. *J. Am. Chem. Soc*. **1990**, *112*, 7389−7390. (b) Yitzchaik, S.; Roscoe, S. B.; Kakkar, A. K.; Allan, D. S.; Marks, T. J.; Xu, Z.; Zhang, T.; Lin, W.; Wong, G. K. *J. Phys. Chem*. **1993**, *97*, 6958−6960. (c) Roscoe, S. B.; Yitzchaik, S.; Kakkar, A. K.; Marks, T. J.; Lin, W.; Wong, G. K. *Langmuir* **1994**, *10*, 1337−1339. (d) Yitzchaik, S.; Marks, T. J. *Acc. Chem. Res*. **1996**, *29*, 197−202.

(7) (a) Katz, H. E.; Scheller, G.; Putvinscki, T. M.; Schilling, M. L.; Wilson, W. L.; Chidsey, C. E. D. *Science* **1991**, *254*, 1485−1487. (b) Katz, H. E.; Wilson, W. L.; Scheller, G. *J. Am. Chem. Soc*. **1994**, *116*, 6636−6640.

(8) (a) Ulman, A. *An Introduction to Ultrathin Organic Films*; Academic Press: New York, 1991; Part 3. (b) Swalen, J. D.; Allara, D. L.; Andrade, J. D.; Chandross, E. A.; Caroff, S.; Israelachvili, J.; McCarthy, T. J.; Murray, R.; Pease, R. F.; Rabolt, J. F.; Wynne, K. J.; Yu, H. *Langmuir* **1987**, *3*, 932−950. (c) Dubois, L. H.; Nuzzo, R. G. *Annu. Rev. Phys. Chem*. **1992**, *43*, 437−463. (d) Bell, C. M.; Yang, H. C.; Mallouk, T. E. In *Materials Chemistry: An Emerging Discipline*; Interrante, L. V., Casper, L. A., Ellis, A. B., Eds.; Adv. Chem. Ser. 245; American Chemical Society: Washington, D.C., 1995; pp 212−230.

(9) (a) Nuzzo, R. G.; Allara, D. L. *J. Am. Chem. Soc*. **1983**, *105*, 4481−4483. (b) Nuzzo, R. G.; Fusco, F. A.; Allara, D. L. *J. Am. Chem. Soc*. **1987**, *109*, 2358−2368. (c) Bain, C. D.; Whitesides, G. M. *Angew. Chem., Int. Ed. Engl*. **1989**, *28*, 506−512. (d) Bain, C. D.; Troughton, E. B.; Tao, Y.-T.; Evall, J.; Whitesides, G. M.; Nuzzo, R. G. *J. Am. Chem. Soc*. **1989**, *111*, 321−335.

(10) (a) Allara, D. L.; Atre, S. V.; Elliger, C. A.; Snyder, R. G. *J. Am. Chem. Soc*. **1991**, *113*, 1852−1854. (b) Allara, D. L.; Nuzzo, R. G. *Langmuir* **1985**, *1*, 45−52.

(11) (a) Wasserman, S. R.; Tao, Y.-T.; Whitesides, G. M. *Langmuir* **1989**, *5*, 1074−1087. (b) Maoz, R.; Sagiv, J. *Langmuir* **1987**, *3*, 1034−1044. (c) Pomerantz, M.; Segmuller, A.; Netzer, L.; Sagiv, J. *Thin Solid Films* **1985**, *132*, 153−162.

(12) (a) Zeppenfeld, A. C.; Fiddler, S. L.; Ham, W. K.; Klopfenstein, B. J.; Page, C. J. *J. Am. Chem. Soc*. **1994**, *116*, 9158−9165. (b) Cao, G.; Hong, H.-G.; Mallouk, T. E. *Acc. Chem. Res*. **1992**, *25*, 420−425. (c) Thompson, M. E. *Chem. Mater*. **1994**, *6*, 1168−1175.

(13) Thoden van Velzen, E. U. Ph.D. Thesis, University of Twente, 1994, Chapter 1.

(14) (a) Lin, W.; Yitzchaik, S.; Lin, W.; Malik, A.; Durbin, M. K.; Richter, A. G.; Wong, G. K.; Dutta, P.; Marks, T. J. *Angew. Chem., Int. Ed. Engl*. **1995**, *34*, 1497−1499. (b) Yitzchaik, S.; Lin, W.; Marks, T. J.; Lin, W.; Wong, G. K. *Polym. Mater. Sci. Eng*. **1995**, *72*, 217−218. (c) Lin, W.; Marks, T. J.; Yitzchaik, S.; Lin, W.; Wong, G. K. *Mat. Res. Soc. Sympos. Proc*., in press. (d) Lin, W.; Malinsky, J. E.; Marks, T. J.; Lin, W.; Wong, G. K. Manuscript in preparation.

(15) Roscoe, S. B.; Kakkar, A. K.; Marks, T. J.; Malik, A.; Durbin, M. K.; Lin, W.; Wong, G. K.; Dutta, P. *Langmuir*, in press.

(16) (a) Moylan, C. R.; Swanson, S. A.; Walsh, C. A.; Thackara, J. I.; Twieg, R. J.; Miller, R. D.; Lee, V. Y. Nonlinear Optical Properties of Organic Materials VI. In *SPIE Proc*. **1993**, *2025*, 192−201. (b) Twieg, R. J.; Burland, D. M.; Hedrick, J. L.; Lee, V. Y.; Miller, R. D.; Moylan, C. R.; Volksen, W.; Walsh, C. A. *Mat. Res. Soc. Sympos. Proc*., in press.

(17) (a) Zhao, X.-M.; Perlstein, J.; Whitten, D. G. *J. Am. Chem. Soc*. **1994**, *116*, 10463−10467. (b) Takagi, K.; Shibata, S.; Oguri, S.; Sawaki, Y.; Suzuoki, Y.; Segi, T. *Chem. Lett*. **1993**, 2103−2106. (c) Usami, H.; Takagi, K.; Sawaki, Y. *J. Chem. Soc., Faraday Trans*. **1992**, *88*, 77−81. (d) Takagi, K.; Suddaby, B. R.; Vadas, S. L.; Backer, C. A.; Whitten, D. G. *J. Am. Chem. Soc*. **1986**, *108*, 7865−7867. (e) Quina, F. H.; Whitten, D. G. *J. Am. Chem. Soc*. **1977**, *99*, 877−883.

(18) After completion of this work, a communication on Langmuir−Blodgett films based on lanthanide salts of the (*E*)-1-methyl-4-[[4-(dihexadecylamino)phenyl]azo]pyridinium chromophore appeared. See: Gao, L. H.; Wang, K. Z.; Huang, C. H.; Zhao, X. S.; Xia, X. H.; Li, T. K.; Xu, J. M. *Chem. Mater*. **1995**, *7*, 1047−1049.

Scheme 1. Synthesis and Purification of the Chromophore Precursor 4-[[4-[*N*,*N*-Bis(hydroxylethyl)amino]phenyl]azo]pyridine, **1**

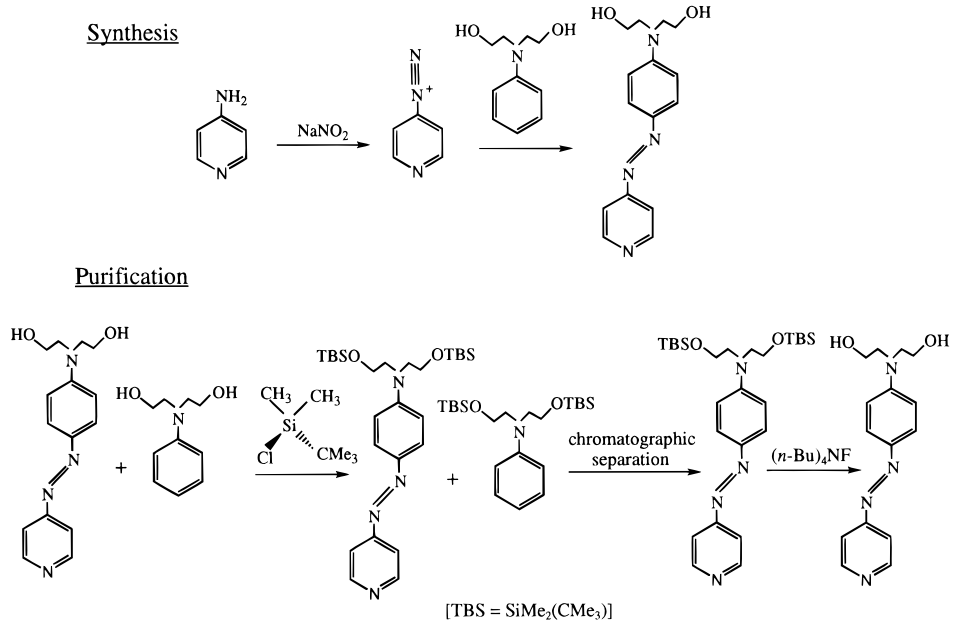

Construction of Chromophoric Superlattices. Sodium lime glass, quartz, or silicon wafer substrates were cleaned by immersion in "piranha" solution at 80 °C for 1 h. After being cooled to room temperature, they were rinsed repeatedly with deionized water and then subjected to an RCA-type cleaning protocol (room temperature, 40 min). They were then washed with deionized water and dried under vacuum immediately before coupling agent deposition.

(i) Self-Assembly of 4-$ClCH_2C_6H_4SiCl_3$. Under inert atmosphere, freshly cleaned glass or silicon single crystal substrates were immersed in a 1:100 (v/v) solution of 4-$ClCH_2C_6H_4SiCl_3$ in heptane for 20 min, washed with pentane, and sonicated in acetone for 1 min. The 3-$BrC_3H_6SiCl_3$ and 3-$IC_3H_6SiCl_3$ coupling layers were chemisorbed similarly.

(ii) Self-Assembly of the 4-[[4-[*N*,*N*-Bis(hydroxylethyl)amino]-phenyl]azo]pyridinium Chromophore. The silylated substrates (after step i treatment) were spin-coated at 4000 rpm with a 5 mM solution of 4-[[4-[*N*,*N*-bis(hydroxylethyl)amino]phenyl]azo]pyridine in methanol inside a class 100 clean hood (Envirco) and then heated at 110 °C in a vacuum oven (0.4 Torr) for 13 min. The samples were cooled to room temperature and then washed with methanol and acetone to remove any residual **1**.

(iii) Self-Assembly of Octachlorotrisiloxane. The glass and silicon single crystal substrates after step i and step ii treatment were immersed in a 1:150 (v/v) solution of octachlorotrisiloxane in heptane for 30 min, washed with pentane, and sonicated in acetone for 1 min.

Physical Measurements. Full details of the physical measurements are given in the supporting information. Polarized second harmonic generation measurements were made in the transmission mode using the 1064 nm output of a Q-switched Nd:YAG laser operated at 10 Hz with a pulse width of 3 ns. The details of this setup can be found elsewhere.[6b] Contact angles were measured on a standard goniometric bench fitted with a Teflon micrometer syringe. X-ray photoelectron spectra were recorded on a VG Scientific Ltd., Escalab MK II instrument. Details of the spectral acquisition and data analysis techniques are described elsewhere.[6c] X-ray reflectivity measurements were performed at Beam Line X23B of the National Synchrotron Light Source. Data acquisition and analysis procedures are described elsewhere.[19] Ellipsometric data were obtained on a Sopra MOSS ES 4 G spectroscopic ellipsometer. The data were modeled in the multilayer regression mode with the number of layers set to 2; a refractive index of 1.7 was assumed for the self-assembled multilayers, while the literature values of the refractive indices for silicon and silicon oxide were used for these materials.[20] Atomic force microscopic images were recorded using a Nanoscope II microscope with A and D scanners (Digital Instruments, Inc.). All of the AFM samples were prepared on Si(100) single crystal substrates having a root mean square (rms) roughness of 2.0 Å.

Results

(1) Synthesis of 4-[[4-[*N*,*N*-Bis(hydroxylethyl)amino]phenyl]azo]pyridine, 1. The new chromophore precursor 4-[[4-[*N*,*N*-bis(hydroxylethyl)amino]phenyl]azo]pyridine was prepared by diazotization of 4-aminopyridine to form a 4-pyridyldiazonium intermediate followed by coupling with *N*-phenyldiethanolamine (Scheme 1). Because the 4-pyridyldiazonium intermediate has very limited stability in solution,[21] it was generated *in situ* and immediately coupled with *N*-phenyldiethanolamine to form **1** in modest yields. The product 4-[[4-[*N*,*N*-bis-(hydroxylethyl)amino]phenyl]azo]pyridine, however, is difficult to separate from the *N*-phenyldiethanolamine starting material. To facilitate this separation, the mixture was treated with *tert*-butyldimethylchlorosilane, which derivatized the hydroxyl groups to siloxy functionalities.[22] The resulting 4-[[4-[*N*,*N*-bis-[(*tert*-butyldimethylsiloxy)ethyl]amino]phenyl]azo]pyridine, **2**, can be easily separated from *N*-phenyl[bis[(*tert*-butyldimethyl-siloxy)ethyl]]amine by chromatography on silica gel with a mixture of hexane and ethyl acetate as the eluant. Compound **2** can be readily transformed back to chromophore precursor **1** by treatment with tetra-*n*-butylammonium fluoride in tetrahydrofuran. Both **1** and **2** have been characterized by elemental analysis, mass spectrometry, and infrared, UV−vis, and NMR spectroscopies (see the supporting information for details). Spectroscopic data for **1** and **2** are consistent with those reported for the related known compound, 4-[[4-(*N*,*N*-dimethylamino)-phenyl]azo]pyridine.[23] The synthesis and purification of **1** are summarized in Scheme 1.

(2) Preparation and Characterization of Self-Assembled [(Aminophenyl)azo]pyridinium Monolayers. As illustrated in Scheme 2, the construction of [(aminophenyl)azo]pyridinium monolayers is based on chemisorptive siloxane self-assembly strategies first developed by Sagiv.[11] Cleaned, hydroxylated substrates such as glass or single-crystal silicon wafers were

(19) Shih, M. C.; Peng, J. B.; Huang, K. G.; Dutta, P. *Langmuir* **1993**, *9*, 776−782.
(20) Collins, R. W.; Allara, D. L.; Kim, Y.-T.; Lu, Y.; Shi, J. In *Characterization of Organic Thin Films*; Ulman, A., Ed.; Butterworth-Heinemann: Boston, 1995; pp 35−55.
(21) Kalatzis, E. *J. Chem. Soc., B* **1967**, 273−277.
(22) Greene, T. W.; Wuts, P. G. M. *Protective Groups in Organic Synthesis*; 2nd ed.; John Wiley & Sons: New York, 1991; pp 77−81.
(23) (a) Kubota, H.; Idei, M.; Motomizu, S. *Analyst* **1990**, *115*, 1109−1115. (b) Pentimalli, L. *Tetrahedron* **1960**, *9*, 194−201.

Scheme 2. Construction of Self-Assembled 4-[[4-[Bis(hydroxylethyl)amino]phenyl]azo]pyridinium multilayers[a]

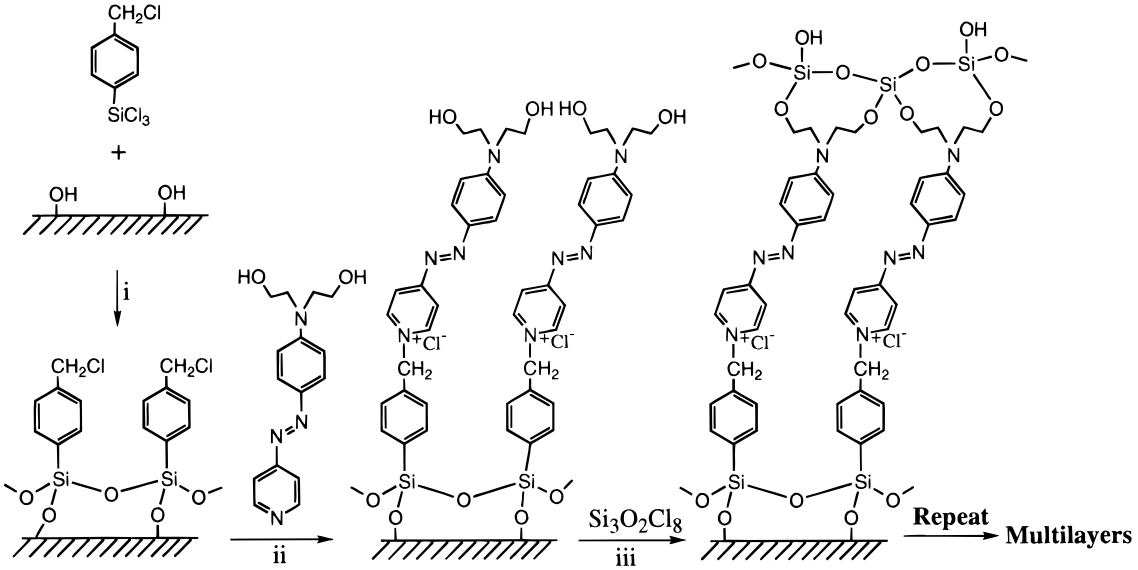

[a] Conditions: step i, 1/100 (v/v) [4-(chloromethyl)phenyl]trichlorosilane in dry heptane for 20 min; step ii, spin-coated from 5 mM CH_3OH solution at 4000 rpm and baked at 110 °C/0.4 Torr for 13 min; step iii, 1/150 (v/v) octachlorotrisiloxane in dry heptane for 30 min.

first treated with 4-$ClCH_2C_6H_4SiCl_3$ to afford a monolayer of coupling agent. The [(aminophenyl)azo]pyridinium chromophore layer was deposited upon this coupling layer via the quaternization of [(aminophenyl)azo]pyridine. Finally, the chromophoric layer was planarized/crosslinked with octachlorotrisiloxane; this step also regenerates hydroxyl groups on which subsequent layers can be iteratively constructed.

(a) Self-Assembled Coupling Layers. Under rigorously anhydrous/anaerobic conditions, the freshly cleaned substrates were treated with a 1:100 (v/v) solution of 4-$ClCH_2C_6H_4SiCl_3$ in dry heptane for 20 min, followed by washing with copious amounts of pentane and acetone to remove physisorbed coupling agent. This treatment (step i, Scheme 2) is known to afford a densely packed, self-assembled monolayer of benzylic chloride coupling agent on the surface.[15] The self-assembled coupling layer was characterized by advancing aqueous contact angle (θ_a) measurements and ellipsometry. The contact angle changes from 15° for SiO_2 to 70° for the silylated surface. This hydrophobic change in θ_a is consistent with the presence of benzylic chloride functionalities on the surface.[24] Ellipsometric measurements reveal a thickness of ~10 Å for the self-assembled coupling agent.[25] This thickness agrees well with that of a self-assembled 4-$ClCH_2C_6H_4SiCl_3$ monolayer reported by Koloski *et al.*[26] and is consistent with that expected for a chemisorbed monolayer of 4-$ClCH_2C_6H_4SiCl_3$ from molecular modeling.

In order to further characterize the self-assembled monolayers using X-ray photoelectron spectroscopy (XPS), monolayers were also prepared using 3-$BrC_3H_6SiCl_3$ and 3-$IC_3H_6SiCl_3$ as coupling agents.[27] XPS spectra of the 3-$BrC_3H_6SiCl_3$-derived coupling layer films exhibit a Br 3d signal at 70.5 eV (Figure 1); this binding energy is consistent with an alkyl bromide moiety.[28] Interestingly, no Cl 2p signal is present in the spectrum, suggesting that the labile Si−Cl bonds have been completely hydrolyzed to form densely packed siloxane linkages on the surface. Similarly, the XPS spectra of the corresponding

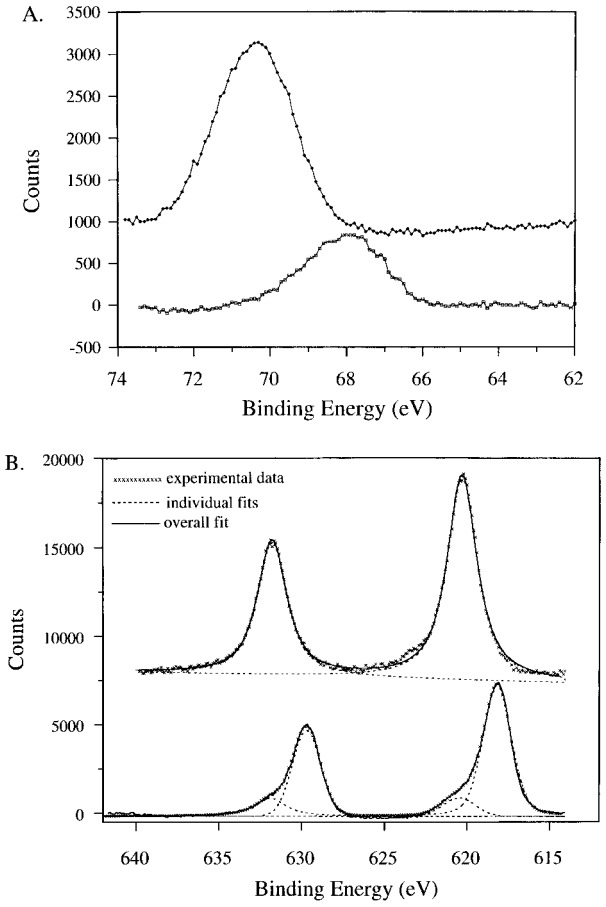

Figure 1. (A) Br 3d XPS spectra of self-assembled 3-$BrC_3H_6SiCl_3$ coupling and [(aminophenyl)azo]pyridinium chromophore monolayers. Bottom spectrum: after coupling agent deposition. Top spectrum: after coupling agent and chromophore deposition. (B) I 3d XPS spectra of self-assembled 3-$IC_3H_6SiCl_3$ coupling and [(aminophenyl)azo]pyridinium chromophore monolayers. Bottom spectrum: after coupling agent deposition. Top spectrum: after coupling agent and chromophore deposition.

(24) Li, D.; Neumann, A. W. In *Characterization of Organic Thin Films*; Ulman, A., Ed.; Butterworth-Heinemann: Boston, 1995; pp 165−192.

(25) All the ellipsometry-derived thicknesses reported in this contribution are, within experimental error, consistent with those derived from independent X-ray reflectivity measurements. Lin, W.; Malik, A.; Malinsky, J. E.; Durbin, M. K.; Dutta, P.; Marks, T. J. Manuscript in preparation.

(26) Koloski, T. S.; Dulcey, C. S.; Haralson, Q. J.; Calvert, J. M. *Langmuir* **1994**, *10*, 3122−3133.

(27) Our previous XPS studies[6c] on ion exchange processes of self-assembled stilbazolium monolayers showed that the complicated Cl 2p line shape resulting from overlap of the Cl $2p_{1/2}$ and Cl $2p_{3/2}$ peaks can complicate the deconvolution of Cl 2p signals and therefore obscure shifts in Cl 2p binding energies.

propyl iodide (3-$IC_3H_6SiCl_3$) coupling layer films exhibit an I $3d_{5/2}$ signal at 620.3 eV, which is also consistent with an alkyl iodide functionality. Thus, these XPS results further support the formation of self-assembled coupling layers.

(b) Self-Assembled [(Aminophenyl)azo]pyridinium Chromophore Layer. The deposition of the [(aminophenyl)azo]-pyridinium chromophore layers has been achieved in a "topotactic" fashion (see the Discussion section).[14] The substrates terminated with a coupling layer were spin-coated with a thin layer (∼500 Å thick) of 4-[[4-[*N*,*N*-bis(hydroxylethyl)amino]-phenyl]azo]pyridine, followed by brief heating in vacuo to effect quaternization and removal of excess chromophore precursor **1** (110 °C/0.4 Torr). These samples were then washed with methanol and acetone to ensure the complete removal of excess **1** on the surfaces. This procedure yields a self-assembled monolayer of the [(aminophenyl)azo]pyridinium chromophore layer via the quaternization of [(aminophenyl)azo]pyridine with the benzylic chloride functionality. This [(aminophenyl)azo]-pyridinium self-assembly process has been monitored by transmission optical spectroscopy, advancing aqueous contact angle measurements, ellipsometry, polarized second harmonic generation, and XPS.

After step ii, the films exhibit three optical absorption maxima at 278, 450, and 573 nm. The new absorption maximum at 573 nm can be assigned to a longitudinal HOMO → LUMO charge transfer excitation in the quaternized [(aminophenyl)-azo]pyridinium chromophore.[29] This result suggests that **1** undergoes quaternization with the benzylic chloride to form a self-assembled monolayer of the 4-[[4-[*N*,*N*-bis(hydroxylethyl)-amino]phenyl]azo]pyridinium chromophore on the surface. This conclusion is further supported by the advancing aqueous contact angle of the surface, which shows the expected hydrophilic change with θ_a falling to 40° upon [(aminophenyl)azo]pyridinium chromophore deposition. Consistent with this observation, ellipsometric measurements also show an increase in film thickness from ∼10 to ∼18 Å after quaternization step ii.

XPS spectra of the chromophoric monolayers with *n*-propyl bromide and *n*-propyl iodide coupling layers provide further evidence for the chemisorptive deposition of the 4-[[4-[*N*,*N*-bis(hydroxylethyl)amino]phenyl]azo]pyridinium chromophore on the surface. Thus, the [(aminophenyl)azo]pyridinium chromophore monolayers with the 3-$BrC_3H_6SiCl_3$ and 3-$IC_3H_6SiCl_3$ coupling agents exhibit optical spectra and SHG responses (*vide infra*) similar to those of the chromophoric monolayers with the 4-$ClCH_2C_6H_4SiCl_3$ coupling layer. In bilayer samples prepared with 3-$BrC_3H_6SiCl_3$ as the coupling agent, the XPS spectrum shows a Br 3d binding energy of 68.0 eV upon the quaternization of **1** (Figure 1A). This 2.5 eV shift to lower binding energy is consistent with the formation of Br^- anions.[28] However, overlap of the Br $3d_{3/2}$ and Br $3d_{5/2}$ peaks precludes the deconvolution of the Br 3d signals, and therefore, it is not straightforward to quantitatively determine the extent of the quaternization process. This difficulty was overcome using 3-$IC_3H_6SiCl_3$ as the coupling agent. Here, the I $3d_{5/2}$ XPS spectrum of the 3-$IC_3H_6SiCl_3$ coupling layer exhibits two distinct peaks upon quaternization (Figure 1B). While the minor peak has a binding energy of 620.3 eV, the major peak has shifted to a lower binding energy of 618.2 eV. These two peaks can be assigned to unquaternized propyl iodide and quaternized iodide anion, respectively. The integration of these two peaks

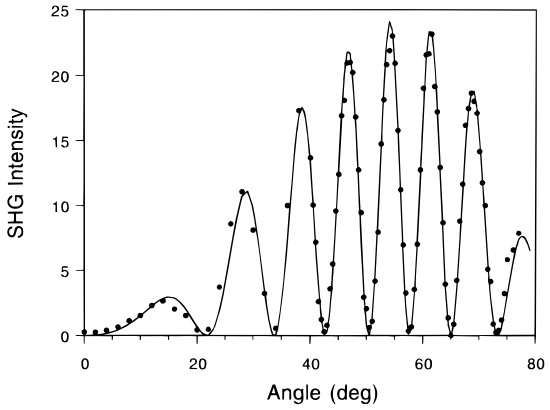

Figure 2. SHG intensity as a function of fundamental light ($\lambda_0 = 1064$ nm) incident angle from a glass slide surface having a self-assembled [(aminophenyl)azo]pyridinium monolayer on both sides. The coupling agent is 4-$ClCH_2C_6H_4SiCl_3$.

provides further information on the quaternization process: the two peaks at 620.3 and 618.2 eV have an intensity ratio of ∼1:9. This indicates that ∼90% of the propyl iodide functionalities comprising the coupling layer have undergone reaction with **1** to form the anchored 4-[[4-[*N*,*N*-bis(hydroxylethyl)amino]-phenyl]azo]pyridinium chromophore on the surface. The presence of the 4-[[4-[*N*,*N*-bis(hydroxylethyl)amino]phenyl]azo]-pyridinium chromophore on the surface can be further inferred from the N 1s XPS spectrum, which shows a broad unsymmetrical peak centered around 400.5 eV. The N 1s signal can be deconvoluted into three peaks with binding energies of 399.4, 400.5, and 402.0 eV.[30] These peaks are assigned to the amino, azo, and pyridinium nitrogen atoms, respectively.[28]

The most convincing evidence for the deposition of aligned 4-[[4-[*N*,*N*-bis(hydroxylethyl)amino]phenyl]azo]pyridinium chromophore molecules comes from polarized second harmonic generation measurements, which show a large increase in the second harmonic response in the quaternized, bilayer film. Such a large second harmonic response can only be explained by the presence of the high-β 4-[[4-[*N*,*N*-bis(hydroxylethyl)amino]-phenyl]azo]pyridinium chromophore chemisorbed onto the surface.[29] Figure 2 shows angle-dependent SHG response data from a sample coated with the 4-[[4-[*N*,*N*-bis(hydroxylethyl)-amino]phenyl]azo]pyridinium chromophore on both sides of the glass substrate, which were prefunctionalized with the 4-$ClCH_2C_6H_4SiCl_3$ coupling agent. Qualitatively similar SHG angle dependence was observed for bilayer samples with the 3-$BrC_3H_6SiCl_3$ and 3-$IC_3H_6SiCl_3$ coupling agents. The characteristic SHG interference pattern in Figure 2 is due to the phase difference between two SHG waves generated at either side of the sample. The presence of near-zero intensity minima in Figure 2 indicates that the quality and uniformity of the monolayers on both sides of the glass substrate are nearly identical. This result provides indirect evidence for the good structural regularity of the chromophoric monolayers prepared with the present self-assembly technique. Furthermore, the experimental angle-dependent SHG data can be analyzed according to literature methods.[31] The solid curve in Figure 2 shows the fit to $\chi^{(2)}_{zzz}/\chi^{(2)}_{zyy} = 3$. Assuming a unidimensional

(28) Moulder, J. F.; Stickle, W. F.; Sobol, P. E.; Bomben, K. D. *Handbook of X-ray Photoelectron Spectroscopy*; Perkin Elmer: Eden Praire, MN, 1992.

(29) ZINDO/SOS calculations show that the HOMO → LUMO charge transfer excitation red-shifts by ∼100 nm as **1** undergoes quaternization to form the [(aminophenyl)azo]pyridinium chromophore. $\beta^{calc}_{vec} = 984 \times 10^{-32}$ cm^5 esu^{-1} ($\lambda_o = 1064$ nm) by the ZINDO/SOS formalism.

(30) We assume that the N1s binding energies of the two azo N atoms of the [(aminophenyl)azo]pyridinium chromophore are sufficiently similar so that only three N1s peaks are expected. We employed the binding energies and linewidths (FWHM) of the N1s peaks of the amino and pyridinium nitrogen atoms of self-assembled stilbazolium monolayers in deconvolution of the present XPS data.[14c]

(31) (a) Ashwell, G. J.; Hargreaves, R. C.; Baldwin, C. E.; Bhara, G. S.; Brown, C. R. *Nature* **1992**, *357*, 393−395. (b) Lupo, D.; Prass, W.; Scheunemann, U.; Laschewsky, A.; Ringsdorf, H. *J. Opt. Soc. Am.* **1988**, *5B*, 300−308.

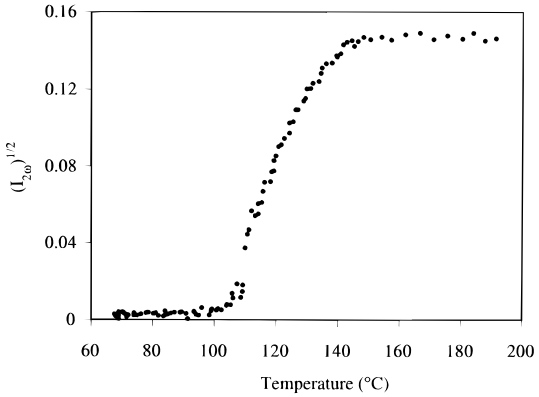

Figure 3. *In situ* monitoring of the quaternization/chromophore chemisorption step ii in Scheme 2 by transmission second harmonic generation at $\lambda_0 = 1064$ nm. The coupling agent is 4-$ClCH_2C_6H_4SiCl_3$. Temperature ramp: 60−150 °C, 1 °C/min; 150−200 °C, 1.5 °C/min.

chromophore (i.e., with a single dominant β tensor component) and minimal dispersion, the average orientation angle of the chromophore dipoles with respect to the surface normal (tilt angle) can then be calculated from the expression $\chi^{(2)}_{zzz}/\chi^{(2)}_{zyy} = 2\cot^2\bar{\psi}$. The tilt angles for the present self-assembled chromophoric superlattices fall in the range of 38−42°, comparing favorably with those calculated for the self-assembled and Langmuir−Blodgett films of a related stilbazolium chromophore.[6,31]

In order to better understand the chromophore self-assembly process, the quaternization step (step ii, Scheme 2) was also studied using an *in situ* SHG technique. In this experiment, glass substrates that had been coated with self-assembled 4-$ClCH_2C_6H_4SiCl_3$ coupling layers were spin-coated with thin layers of **1** and placed in the path of the Nd:YAG laser. The second-harmonic generation responses of these samples were then measured *in situ* while the temperature was ramped at various rates. Figure 3 shows that the onset temperature for chemisorptive chromophore formation is ∼110 °C. The quaternization of 4-[[4-[*N*,*N*-bis(hydroxylethyl)amino]phenyl]azo]-pyridine by the benzylic chloride functionality is quite facile under these conditions. Figure 3 also shows that the quaternization process is complete by ∼140 °C and that the resulting monolayer is stable up to 190 °C in air under these conditions.

(c) Chromophore Surface Density Calculations. By calibrating the SHG data against quartz, a bulk second-order nonlinear susceptibility $\chi^{(2)}_{zzz}$ of 5×10^{-7} esu is obtained for the self-assembled [(aminophenyl)azo]pyridinium bilayers. Chromophore surface densities (N_s) in these bilayers can then be estimated from the surface NLO susceptibilities and the calculated molecular hyperpolarizability β^{calcd}_{zzz} (at 1064 nm) using eq 1.[6b,c,32] The surface susceptibility $(\chi^{(2)}_s)_{\perp\perp\perp}$ is the

$$(\chi^{(2)}_s)_{\perp\perp\perp} = N_s \cos^3\bar{\psi}\,\beta^{calcd}_{zzz} \qquad (1)$$

product of bulk nonlinear optical susceptibility $\chi^{(2)}_{zzz}$ and the bilayer thickness. Using the ZINDO-derived β^{calcd}_{zzz} value of 983.70×10^{-32} esu at 1064 nm, an average tilt angle of 40°, and an estimated bilayer thickness of 18 Å, the chromophore surface density is calculated to be $\sim 2.0 \times 10^{14}$ molecules/cm^2. This value corresponds to an average area ("footprint") of 49 Å^2/molecule, which is in agreement with experimental results from standing wave X-ray fluorescence measurements[33] as well as with that predicted by molecular modeling for a regular self-assembled bilayer. This surface coverage also compares favorably with that determined for LB films containing similar stilbazolium chromophores.[31a] The calculated chromophore surface density of the present system is significantly larger than that derived for the self-assembled stilbazolium bilayers prepared using earlier solution phase deposition techniques ($\sim 1.1 \times 10^{14}$ molecules/cm^2).[6b] This result suggests that the "topotactic" pathway provides greater structural regularity/packing densities in the self-assembled [(aminophenyl)azo]pyridinium monolayers so that a greater number of chromophore molecules can be accommodated per unit area.

(d) Self-Assembled Capping Layers. The final (capping) step of the deposition sequence (step iii in Scheme 2) involves treatment of the chromophoric bilayers with octachlorotrisiloxane. This capping step provides lateral structural stabilization/planarization via interchromophore cross-linking and also regenerates hydroxyl groups for the subsequent iterative superlattice assembly process. The deposition of capping layers yields the expected hydrophilic change in θ_a; the advancing aqueous contact angle of the surface decreases from 40° to 17° after capping layer chemisorption. This result is consistent with the regeneration of surface hydroxyl groups as a result of the capping layer deposition. Ellipsometric measurements show that the thickness of the film after capping layer deposition has increased to ∼25 Å.

(3) Synthesis and Characterization of Self-Assembled [(Aminophenyl)azo]pyridinium Multilayer Films. The construction of self-assembled multilayers involves repetitive deposition of the aforementioned coupling, chromophore, and capping layers (Scheme 2). The present "topotactic" approach has very high efficiency: the total reaction time for constructing a complete trilayer is about 1 h. The degree to which the present self-assembly approach produces a regular superlattice without loss of acentricity (randomization of chromophore orientation) and diminution of SHG efficiency was investigated as a function of the number of added layers (steps i−iii) by ellipsometry, X-ray reflectivity, transmission optical spectroscopy, and SHG.

Figure 4 shows the dependence of ellipsometry- and X-ray reflectivity-derived multilayer thicknesses on the number of trilayers. The superlattice thicknesses exhibit a smooth, monotonic increase as a function of the total number of assembled layers. The ellipsometric measurements give a thickness of ∼25 Å for each trilayer, while the X-ray reflectivity measurements give a trilayer thickness of 24.2 ± 1 Å. The inset of Figure 4 shows the X-ray reflectivity data for a 10-trilayer self-assembled [(aminophenyl)azo]pyridinium multilayer film. The closely spaced minima in the data are due to the interference between the reflections from the film−substrate and film−air interfaces, from which the thickness of the 10-trilayer film is determined to be 240 ± 1 Å. This thickness is further supported by the appearance of the Bragg peak at $K_z = 0.24$ Å^{-1}, which is due to scattering from individual layers; the interlayer spacing calculated from this peak position is 24 ± 1 Å. The detailed analyses of these X-ray reflectivity data will be reported elsewhere.[19,25] Considering the differences in radiation wavelength as well as in analysis assumptions and procedures, the ellipsometric and X-ray reflectivity film thickness results can be considered to be in good agreement. The linear dependence of multilayer thicknesses (determined from both spectroscopic ellipsometry and X-ray reflectivity) on the number of assembled

(32) Heinz, T. F.; Tom, H. W. K.; Shen, Y. R. *Phys. Rev. A* **1983**, *28*, 1883−1885.

(33) We have recently measured the surface Br coverage of the self-assembled stilbazolium monolayers using standing wave X-ray fluorescence techniques at NSLS. The surface Br coverage is on the order of 40−50 Å^2/atom. Lin, W.; Lee, T.-L.; Lyman, P. F.; Lee, J.; Bedzyk, M. J.; Marks, T. J., submitted for publication.

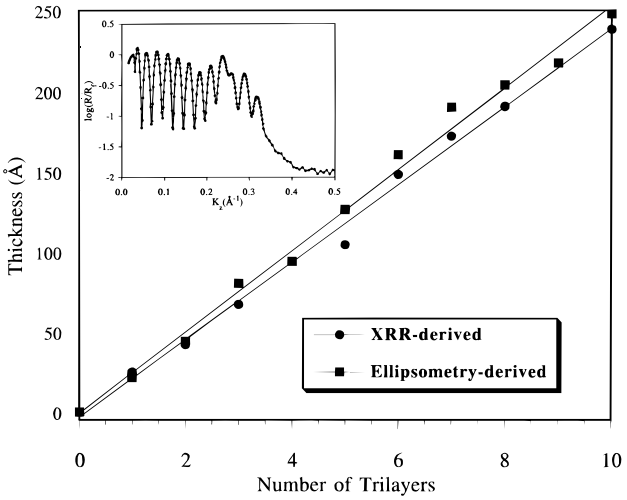

Figure 4. Ellipsometry- and X-ray reflectivity-derived thicknesses for the self-assembled chromophoric multilayers of Scheme 2 as a function of the number of trilayers. The inset shows the X-ray reflectivity data for a 10-trilayer self-assembled chromophoric multilayer. Each trilayer is composed of the sequence steps i−iii. The coupling agent is 4-$ClCH_2C_6H_4SiCl_3$.

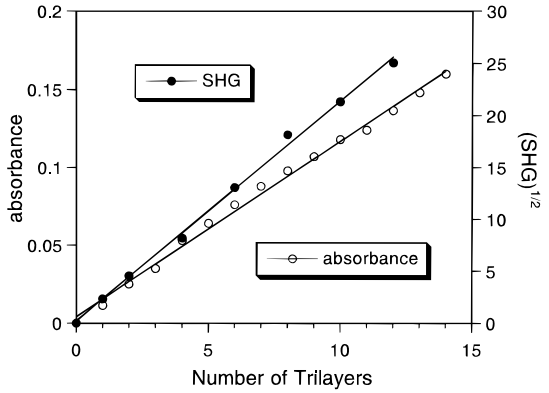

Figure 5. Optical absorbance at 572 nm and square root of the 532 nm second harmonic generation intensity ($\lambda_0 = 1064$ nm) for the self-assembled chromophoric multilayers of Scheme 2 as a function of the number of trilayers. Each trilayer is composed of the sequence steps i−iii. The coupling agent is 4-$ClCH_2C_6H_4SiCl_3$.

trilayers is consistent with the uniform buildup of the chromophoric superlattices.

Further evidence for the buildup of regular superlattice layers comes from the linear dependence of the 572 nm optical absorbance on the number of assembled trilayers (Figure 5). The absorption maximum at 572 nm is assigned to the [(aminophenyl)azo]pyridinium chromophore longitudinal HOMO → LUMO charge-transfer excitation.[29] This linear dependence suggests that equal amounts of chromophore are deposited in constructing each trilayer and that a uniform chromophore orientation is maintained in the self-assembled multilayers.

A final test of superlattice regularity comes from the SHG response as a function of the number of trilayers. Because the film thicknesses are small compared to the wavelength of the incident light, the intensity of the SHG light from a regular multilayer structure should scale quadratically with the number of trilayers. The observed linear dependence of the square root of the SHG intensity on the number of trilayers indicates both structural regularity in layer thicknesses as well as uniform alignment of the chromophore molecules (Figure 5). From the slope, $\chi^{(2)} \sim 3.6 \times 10^{-7}$ esu (∼150 pm/V) can be deduced (we take the chromophoric trilayer thickness to be 25 Å); this is slightly lower than the aforementioned monolayer result (*vide supra*) due to the added thickness imparted by the siloxane layer introduced in step iii. This level of second-order nonlinearity is comparable to or greater than those of the most optically nonlinear siloxane and zirconium phosphonate/phosphate self-assembled chromophoric multilayers reported to date.[6,7,14] The SHG efficiency of the self-assembled [(aminophenyl)azo]-pyridinium multilayers also rivals those of the most efficient poled polymers and LB films reported to date.[1,2,5]

We also carried out initial photostability studies on the self-assembled [(aminophenyl)azo]pyridinium multilayers. It is found that the second harmonic response of the [(aminophenyl)-azo]pyridinium multilayers exhibits negligible decay after exposure to fluorescent light for over 1 month. It is reasonable that the photostability is mainly a result of the resistance of the azo linkage to degradative [2 + 2] cycloaddition or oxidative processes that would yield SHG-inactive products.[17]

(4) Atomic Force Microscopy Studies. Atomic force microscopy has proven to be a powerful technique for determining molecular scale ordering of Langmuir−Blodgett films[34] and self-assembled monolayers.[35] The microstructural regularity of the monolayers can be inferred from the surface morphologies of these samples. To our knowledge, however, there have been only two atomic force microscopic studies of self-assembled metal phosphonate multilayers,[36] and no AFM study on self-assembled siloxane multilayers has been reported. This is presumably due to the lack of synthetic approaches to these structures. The present multilayer systems provide an interesting opportunity for atomic force microscopic investigations of siloxane-based self-assembled multilayers.

Figure 6A shows an AFM image of a 4-$ClCH_2C_6H_4SiCl_3$ self-assembled monolayer. The coupling layer surface is essentially featureless with an rms roughness of 3.5 Å for a scan area of 1 × 1 μm^2. In comparison, the AFM image of the cleaned Si-(100) substrate (not shown) exhibits an rms roughness of 2.0 Å. In contrast to the growth of self-assembled long chain *n*-alkyltrichlorosilane films,[35a] the 4-$ClCH_2C_6H_4SiCl_3$ monolayers prepared by the present procedure give no evidence by AFM of island growth, and the film morphologies do not appear to depend on the reaction times. This discrepancy is probably because the growth rate for 4-$ClCH_2C_6H_4SiCl_3$ monolayers is very rapid. For example, a complete layer of 4-$ClCH_2C_6H_4$-$SiCl_3$ can be deposited in less than 20 min under the present conditions as judged from the SHG response; in contrast, we find that a complete layer of 4-$ClCH_2C_6H_4C_2H_4SiCl_3$ can only be achieved after 24 h reaction.

An AFM image for a self-assembled [(aminophenyl)azo]-pyridinium bilayer prepared with a 4-$ClCH_2C_6H_4SiCl_3$ coupling layer is shown in Figure 6B. The film is also almost featureless, and the rms roughness has increased only slightly to 4.0 Å. After the deposition of the octachlorotrisiloxane capping layer, the films show essentially the same surface morphology with an rms roughness of ∼5 Å. The most impressive image, however, is that shown in Figure 6C that illustrates the surface morphology of a 10-trilayer (30 layer) self-assembled [(ami-

(34) (a) Meyer, E.; Howald, L.; Overney, R. M.; Heinzelmann, H.; Frommer, J.; Guntherodt, H.-J.; Wagner, T.; Schier, H.; Roth, S. *Nature* **1991**, *349*, 398−400. (b) Weisenhorn, A. L.; Egger, M.; Ohnesorge, F.; Gould, S. A. C.; Heyn, S.-P.; Hansma, H. G.; Sinsheimer, R. L.; Gaub, H. E.; Hansma, P. K. *Langmuir* **1991**, *7*, 8−12.

(35) (a) Bierbaum, K.; Grunze, M.; Baski, A. A.; Chi, L. F.; Schrepp, W.; Fuchs, H. *Langmuir* **1995**, *11*, 2143−2150. (b) Caldwell, W. B.; Campbell, D. J.; Chen, K.; Herr, B. R.; Mirkin, C. A.; Malik, A.; Durbin, M. K.; Dutta, P.; Huang, K. G. *J. Am. Chem. Soc.* **1995**, *117*, 6071−6081. (c) Fujii, M.; Sugisawa, S.; Fukada, K.; Kato, T.; Shirakawa, T.; Seimiya, T. *Langmuir* **1994**, *10*, 984−987. (d) Alves, C. A.; Smith, E. L.; Porter, M. D. *J. Am. Chem. Soc.* **1992**, *114*, 1222−1227.

(36) (a) Yang, H. C.; Aoki, K.; Hong, H.-G.; Sackett, D. D.; Arendt, M. F.; Yau, S.-L.; Bell, C. M.; Mallouk, T. E. *J. Am. Chem. Soc.* **1993**, *115*, 11855−11862. (b) Byrd, H.; Snover, I. L.; Thompson, M. E. *Langmuir* **1995**, *11*, 4449−4453.

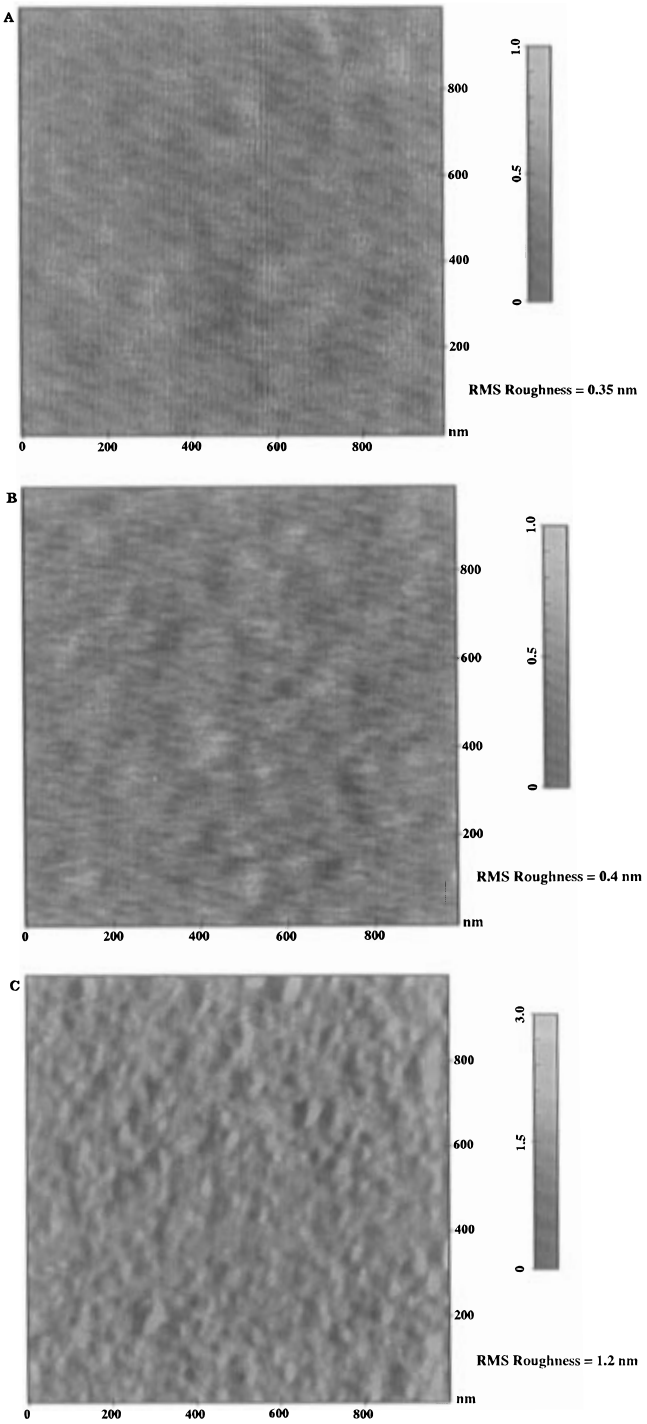

Figure 6. AFM images at 1 × 1 μm^2 scan area of **1**-based self-assembled chromophoric mono- and multilayers. (A) Self-assembled monolayer composed of 4-$ClCH_2C_6H_4SiCl_3$ coupling agent. (B) Self-assembled bilayer composed of 4-$ClCH_2C_6H_4SiCl_3$ coupling agent and 4-[[4-[bis(hydroxylethyl)amino]phenyl]azo]pyridinium chromophore. (C) A 10-trilayer [(aminophenyl)azo]pyridinium chromophore multilayer. Each trilayer is composed of the sequence steps i−iii. The coupling agent is 4-$ClCH_2C_6H_4SiCl_3$.

nophenyl)azo]pyridinium multilayer sample. Although evenly distributed features are evident on the surface, the surface rms roughness is only 12 Å. Considering that such a 10-trilayer sample has an average vertical thickness of 250 Å, the 12 Å average thickness variation (≤5%) is rather small. Unfortunately, this result is not informative in comparing the morphologies of the present multilayers to those of metal phosphonate multilayers on gold substrates. In the latter, surface roughness could not be estimated because of the polycrystalline nature of the gold substrates.[36a] Nonetheless, the AFM results clearly demonstrate that the present multilayers have very smooth surfaces as a result of the high structural regularity within each individual layer.

Discussion

Efficient "Topotactic" Deposition of the [(Aminophenyl)-azo]pyridinium Chromophore. Our previous studies on the solution phase deposition of stilbazolium chromophores indicated that the rate-limiting step in the multilayer deposition process is the chromophore precursor quaternization step (step ii, Scheme 2). For example, a complete layer of the stilbazolium chromophore can only be deposited after 100 h of reaction at typical reagent concentrations and 60 °C. Moreover, long reaction times can result in significant side reactions of the chromophore precursor. Adsorption of these contaminants onto the coupling agent-terminated surfaces results in films with diminished structural regularity and second-order optical nonlinearity. The efficient "topotactic" approach reported here dramatically increases the rate of the chromophore deposition and results in self-assembled chromophoric films with greatly enhanced structural regularity and second-order optical nonlinearity.

In contrast to the previous slow solution phase deposition of the stilbazolium chromophore, the present assembly of the [(aminophenyl)azo]pyridinium chromophore illustrates the great advantage of the "topotactic" multilayer self-assembly approach (which is also applicable to the stilbazolium system).[14] In this new methodology, the substrates terminated with coupling layers are spin-coated with a thin layer of chromophore precursor **1** and then briefly heated at 110 °C under vacuum. UV−vis, XPS, SHG, advancing contact angle measurements, and thickness data all indicate that a complete layer of [(aminophenyl)azo]-pyridinium chromophore can be deposited in each cycle of this procedure. We hypothesize that the ease of the quaternization reaction of **1** is a result of several factors including higher effective concentration of **1** on the surface, higher deposition temperatures, and adequate mobility of **1** on the surface.

Because chromophore preccursor **1** is spin-coated on the surface at high speed (4000 rpm), crystallization of **1** as a result of solvent evaporation is greatly depressed and uniform coverage of **1** on the surface becomes possible. This drastically increases the effective surface concentration of **1** as compared to the solution deposition, which is inevitably limited by the modest solubility of **1**.[37] Equally importantly, higher deposition temperatures become possible because the quaternization step is solvent-free in the present approach. Higher deposition temperatures accelerate the quaternization process. The mobility of **1** on the surface under deposition conditions may also play a significant role in the [(aminophenyl)azo]pyridinium chromophore assembly process. Thermal gravimetric analysis shows that **1** is volatile under the multilayer deposition conditions. Therefore, the facile assembly of the [(aminophenyl)azo]-pyridinium chromophore may be in part due to the gas−surface reaction between **1** and self-assembled coupling agents. However, an alternative interfacial solid state reaction in which the presence of the coupling agent lowers the melting point and enhances the mobility of **1** seems more likely to be the predominant self-assembling pathway. Thus, in situ SHG experiments carried out at atmospheric pressure indicate that the onset temperature for quaternization is ∼110 °C, which is considerably lower than the melting point of **1**, 150.3 °C. Because any volatization process should play at most a minor

(37) Although higher solubility is obtainable in polar solvents, significant side reactions of the chromophore occur, which in turn result in multilayers with diminished structural regularity and second-order response. See: Yitzchaik, S.; Kakkar, A. K.; Roscoe, S. B.; Orihashi, Y.; Marks, T. J.; Lin, W.; Wong, G. K. *Mol. Cryst. Liq. Cryst.* **1994**, *240*, 9−16.

role under these conditions, the ease of the quaternization reaction of **1** on the silylated surface at temperatures below the melting of **1** is more reasonably explained in terms of an interfacial solid state reaction. As a result of the "topotactic" nature of the aminophenylazopyridinium chromophore deposition, the present self-assembly approach has very high efficiency: the total reaction time for constructing a complete trilayer is about one hour.

Structural Regularity of Self-Assembled [(Aminophenyl)azo]pyridinium Superlattices. As mentioned in the Introduction, efficient routes to structurally regular self-assembled multilayers are sparse. The expeditious assembly of the present mutlilayer system enables us to examine the characteristics of reaction chemistry, film uniformity, and microstructural acentricity of the self-assembled superlattices using a variety of spectroscopic and structural techniques.

The combination of UV−vis and XPS spectroscopies indicates that the degree of surface quaternization of chromophore precursor **1** (to form anchored [(aminophenyl)azo]pyridinium chromophore) is ∼90% of the available surface alkyl halide groups. This extent of quaternization is entirely reasonable since the [(aminophenyl)azo]pyridinium chromophore molecule is considerably larger than the 3-$IC_3H_6SiCl_3$ coupling agent, and complete quaternization of the packed surface propyl iodide groups does not appear physically (sterically) reasonable. Interestingly, because the subsequent capping step (step iii, Scheme 2) cross-links/planarizes the surface, any "defect" caused by incomplete conversion in the quaternization step will not catastrophically propagate. We will return to this point later.

The uniform growth of the self-assembled multilayers is indicated by the linear dependence of the [(aminophenyl)azo]-pyridinium chromophore longitudinal HOMO → LUMO charge-transfer absorbance at 572 nm on the number of assembled trilayers as well as by the linear dependence of the ellipsometry- and X-ray reflectivity-derived multilayer thicknesses on the number of assembled trilayers. The most impressive feature, however, is the presence of "Bragg" peaks in the multilayer film XRR data. These features are due to scattering by the individual superlattice layers. The presence of the "Bragg" peaks necessarily requires that the individual layers have similar spacings as well as electron density profiles, both of which are a result of structural uniformity of the multilayers.[38] The mutlilayer structural uniformity is further evidenced in the AFM images that show that the present multilayer films have very smooth surface morphologies.

The most important issue concerns the microstructural acentricity of the multilayer films, because noncentrosymmetric organization is a prerequisite for bulk second-order nonlinear optical effects. The quadratic dependence of the SHG response of the multilayers on the number of assembled trilayers clearly indicates that microstructural acentricity is maintained in the multilayer films. It is reasonable to propose that the "self-annealing" nature of the siloxane capping step (step iii, Scheme 2) in large part assists in stabilizing the microstructural acentricity. In fact, previous studies of self-assembled stilbazolium multilayers have indicated that this structural stabilization/planarization step is crucial in maintaining the acentricity of the chromophore microstructure in the resulting multilayers.[14c] Although XRR and optical spectroscopy indicates the uniform build-up of the stilbazolium chromophoric superlattice when capping step iii is omitted, the intensity of SHG response no longer depends quadratically on the number of layers. As the number of layers exceeds three, the SHG intensity begins to decline. We attribute this fall to the loss of microstructural acentricity as a result of randomization of chromophore alignment, perhaps induced by chromophore dipole−dipole repulsions. In this respect, the present system offers advantages over SHG-active zirconium phosphate/phosphonate assemblies developed by Katz and co-workers. In this only other known self-assembled SHG-active multilayer material, the aforementioned "self-healing" step is not implemented and other measures are needed to produce defect-free, regular structures.[39]

(38) If interlayer spacings and/or electron density profiles vary significantly from trilayer to trilayer, destructive interference will occur. Consequently, no Bragg diffraction peaks will be present in the X-ray reflectivity curves.

Conclusions

We have successfully fabricated regular superlattices containing [(aminophenyl)azo]pyridinium second-order nonlinear optical chromophore using siloxane self-assembly techniques. The [(aminophenyl)azo]pyridinium multilayers can be assembled on hydroxylated substrates in an efficient, "topotactic" fashion via the iterative reaction sequence of a coupling layer, a chromophore layer, and a capping layer. The [(aminophenyl)azo]-pyridinium mono- and multilayers have been characterized by X-ray photoelectron and transmission optical spectroscopies, spectroscopic ellipsometry, X-ray reflectivity, advancing contact angle measurements, and polarized second harmonic generation (SHG) measurements. These spectroscopic and structural data indicate that the [(aminophenyl)azo]pyridinium multilayers have very good structural regularity and very high second-order nonlinear optical susceptibility ($\chi^{(2)} \sim 3.6 \times 10^{-7}$ esu or 150 pm/V at $\omega_0 = 1064$ nm). Atomic force microscopy also reveals that the [(aminophenyl)azo]pyridinium multilayers have very smooth surface morphologies as a result of the high structural regularity. These multilayers are photochemically stable and thermally robust. Because these self-assembled chromophoric superlattices are intrinsically acentric, i.e., no electric-field poling is required to establish bulk second-order nonlinearity (as in poled polymer SHG materials), integration of these self-assembled SHG materials into other device structures should be possible. We are currently pursuing the fabrication of active devices such as low-loss planar waveguides for frequency doubling using self-assembled chromophoric multilayers.[40] We are also extending the present synthetic methodologies to the preparation of other heterostructural assemblies.

Acknowledgment. This research was supported by the NSF through the Northwestern Materials Research Center (DMR9120521) and by the Office of Naval Research. We thank Dr. A. Israel for ZINDO/SOS calculations of linear and nonlinear optical properties of the chromophores, A. Malik, J. Malinsky, and Prof. P. Dutta for assistance with the X-ray reflectivity measurements, and S. Roscoe and Dr. S. Yitzchaik for helpful discussions. W.B.L. thanks the National Science Foundation for a postdoctoral fellowship.

Supporting Information Available: Full experimental details regarding synthesis and physical measurements (6 pages). This material is contained in many libraries on microfiche, immediately follows this article in the microfilm version of the journal, and can be ordered from the ACS; see any current masthead page for ordering information.

JA960395F

(39) Schilling, M. L.; Katz, H. E.; Stein, S. M.; Shane, S. F.; Wilson, W. L.; Buratto, S.; Ungashe, S. B.; Taylor, G. N.; Putvinski, T. M.; Chidsey, C. E. D. *Langmuir* **1993**, *9*, 2156−2160.

(40) (a) Lundquist, P. M.; Lin, W.; Yitzchaik, S.; Wong, G. K.; Marks, T. J. *Appl. Phys. Lett.* in press. (b) Yitzchaik, S.; Lundquist, P. M.; Lin, W.; Wong, G. K.; Marks, T. J. *SPIE Proc.* **1995**, *2285*, 282−289.